Optimization of LETG/HRC-S Spectral Extractions

Brad Wargelin and Pete Ratzlaff

Harvard-Smithsonian Center for Astrophysics/CXC

Abstract

We describe our analysis of the wavelength-dependent cross-dispersion profile of Chandra LETG/HRC-S spectra, which allows the use of a narrower spectral extraction region. Background is reduced by 20% with negligible loss of X-ray signal. Some features of this work are improved 0th order positions, corrections for a fixed pattern of wiggles and slight time-dependent tilts in dispersed spectra, and an updated calibration of the enclosed energy fraction (EEFRAC) that includes the effects of asymmetric cross-dispersion profiles.

1. Helpful Terms and Numbers

- Transmission Grating axes run along (tg_r) and perpendicular to (tg_d) the dispersion axis. tg angles are measured in degrees.
- HRC pixels are 6.4294 μm.
- 1 pixel = 4.265e-05 degrees (tg coordinates).
- 1 tap = 256 pixels = 1.88893 Å in the dispersion direction.
- Coarse tap axes run along (crsv) and perpendicular to (crsu) the dispersion axis.
- The active region of the HRC-S runs from crsv = 6 to 191.
- Low crsv corresponds to HRC-S plate+1 and positive wavelengths. High crsv corresponds to plate-1 and negative wavelengths.
- For on-axis sources, LETG/HRC-S covers about -161 to $+175$ Å.

2. Introduction

The LETG/HRC-S spectral extraction region has a 'bow tie' shape, narrow in the middle and widening beyond $\sim$60 Å to accommodate the inherent astigmatism of the LETG's Rowland-circle geometry. The current extraction region is based on raytrace simulations (see Figure 1) and is somewhat conservative in order to allow for deviations from the idealized model. Our work aims to quantify and, when possible, correct these deviations so that a narrower extraction region can be used, preserving the X-ray extraction efficiency while reducing the number of included background events. We use bright, frequently observed continuum sources to provide complete wavelength coverage with high signal, primarily Mkn421 and PKS2155 for short wavelengths (< 60 Å) and HZ43 for longer wavelengths. We find that:

- Pipeline determinations of zeroth order may have errors of up to $\sim$0.5 pixel. (An improved algorithm is now used in the Pipeline.)
- The cross-dispersion profile (along the tg_d axis) is asymmetric.
- Spectra have a slight time-dependent tilt (up to 4-pixel errors at the ends).
- Spectra have a slight (< 0.5 pixel) time-dependent curvature.
- In addition to tilt, curvature, and slight offsets, dispersed spectra have a time-independent pattern of tg_d offsets ($\sim$2.5 pixels peak-to-peak 'wiggles') as a function of position on the detector.
- Even when 0th order is well positioned and tilt and wiggles have been removed, spectra may be slightly ($\sim$0.5 pixel) offset in tg_d, particularly on the outer plates.

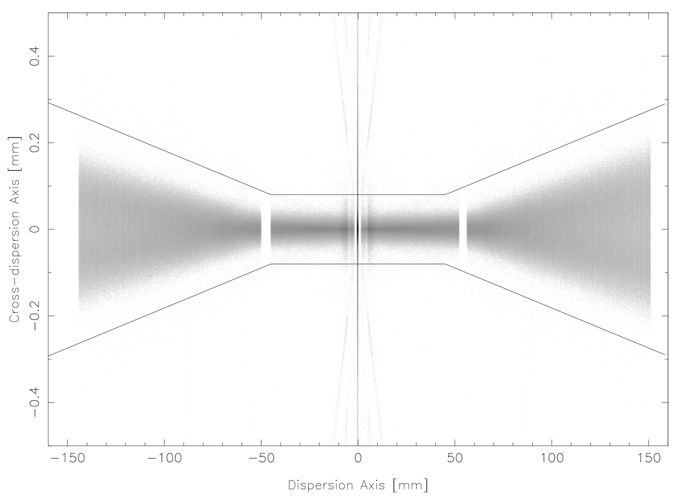

Figure 1: *MARX simulation of a flat spectrum and the current spectral extraction region. Note that the vertical axis is highly stretched. The faint nearly vertical 'whiskers' in the middle are cross-dispersed orders from the LETG fine support structure. About 10% of the total dispersed flux lies in cross-dispersion orders with another $\sim$5% lost to scattering or the extreme wings of the cross-dispersed line spread function, so that the net spectral extraction efficiency of the region shown is $\sim$85%.*

3. Time-Dependent Tilts

After applying pulse-height (PI) background filtering to each observation and removing periods of background flaring we bin the data in the dispersion direction by tap (256 pixels, 1.8889 Å) and in the cross-dispersion direction (tg_d) by 0.00005 to 0.00010 degrees (1.2 to 2.4 pixels), depending on wavelength. We then determine the median of the cross-dispersion profile. Results are plotted in Figure 2. As can be seen, many spectra are slightly tilted. Those tilts, along with those from Capella data, are plotted versus time in Figure 3.

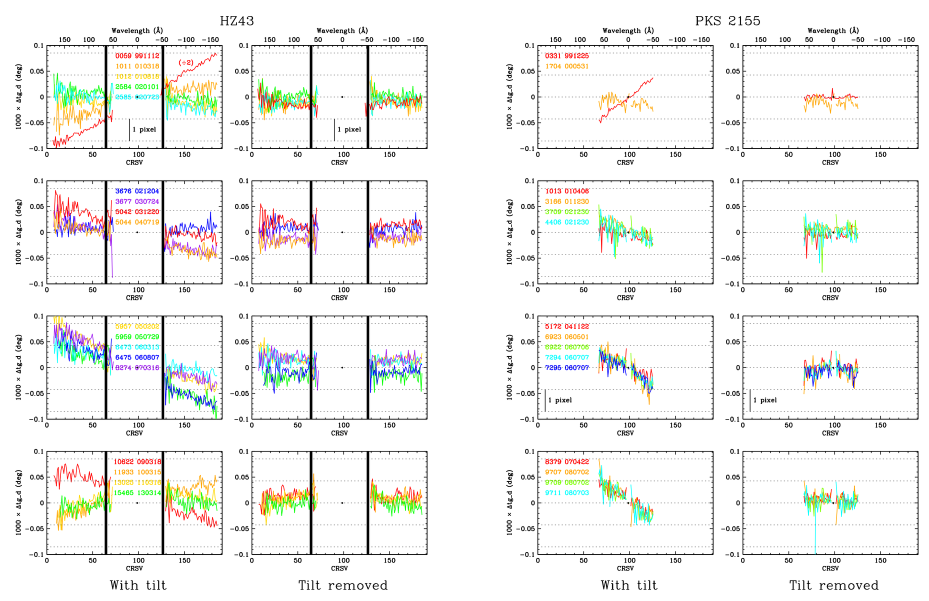

Figure 2: *Median tg_d vs. crsv, after subtracting the average tg_d median for each source. Tilts are therefore relative to the average tilt for each source. For continuum sources, only points with errors of less than 0.00001 degrees (about 1/4 pixel) are plotted. Errors for Capella's lines' medians are explicitly shown.*

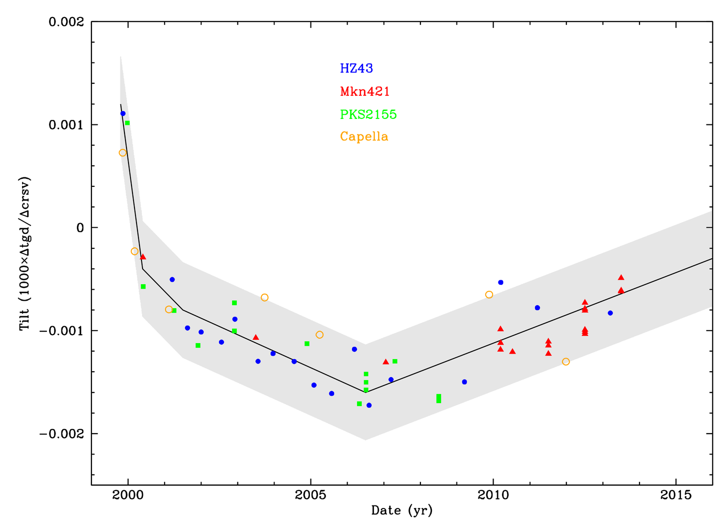

Figure 3: *Spectral tilts versus time. Uncertainties on each point (other than for Capella) are small, so the observed scatter is real and probably caused by observation-specific thermal conditions. There is no apparent correlation with aimpoint jumps. The solid black line can be used to estimate the tilt in any observation, and the gray band denotes the degree of uncertainty that would cause a 1-pixel error at 170 Å.*

4. Time-Independent Wiggles

After correcting for the time-dependent tilts we examined residuals in the tg_d medians and found that the residuals were constant for each source. Figure 4 shows the residuals, or 'wiggles', across the complete wavelength range after applying small adjustments to obtain consistency where spectra overlap.

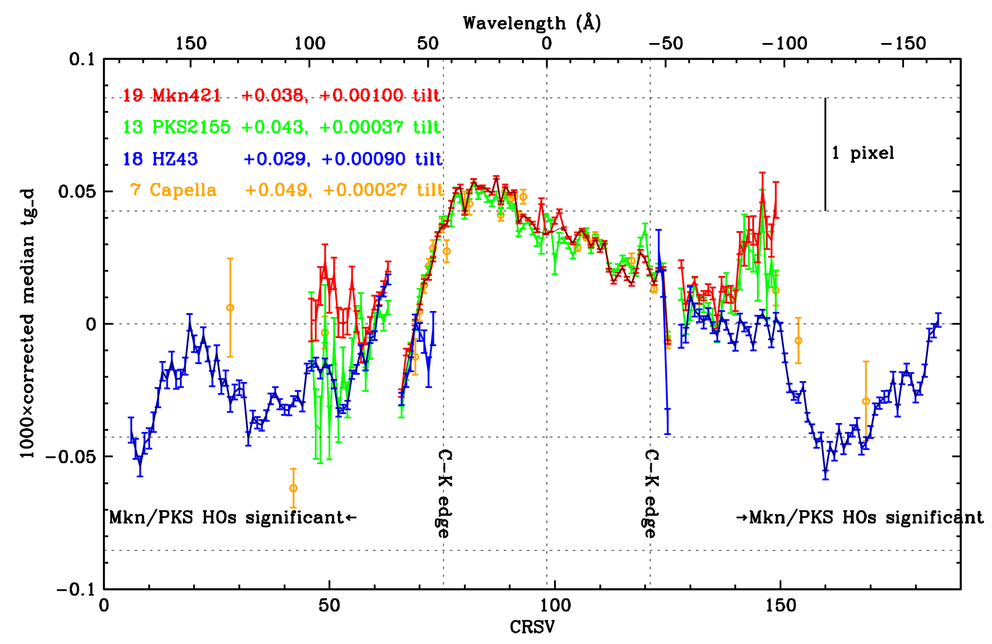

Figure 4: *Median tg_d values for combined spectra, with tilt and offset adjustments to make the wiggle symmetric about tg_d=0. tg_d values are multipled by 1000 for convenience and units are degrees. Tilts are in units of degrees per tap, also multipled by 1000. Legend example: blue points are for 18 combined HZ43 spectra, with a tilt correction of 0.00090 and global offset of 0.043. The composite wiggle curve is shown in black; some points near 0th order and the ends of the inner plate were adjusted by hand because the true errors are larger than indicated by the purely statistical error bars. Outlier points around $\pm$80 Å are caused by higher orders in Mkn421 and PKS2155 spectra, which broaden the observed (1st plus higher orders) profile.*

5. Profile Asymmetry

After correcting for spectral tilts and wiggles we studied the cross-dispersion profiles of the composite spectra. Figures 5 and 6 provide different illustrations of those profiles, which are obviously asymmetric. We are currently calibrating those profiles in order to derive improved enclosed energy fractions (EEFRACs) and define a new, optimized spectral extraction region. Our hope is to narrow the region by 20–25%, reducing the included background by the same amount, with only a tiny change (< 1%) in X-ray extraction efficiency. Preliminary EEFRAC results (normalized to the total flux on the detector, rather than 2π as will be needed for the CALDB EEFRAC table) are shown in Figure 7.

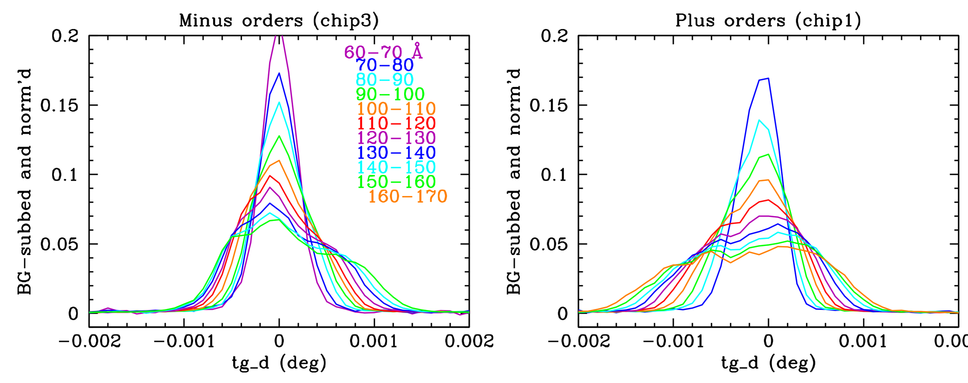

Figure 5: *tgd profiles for HZ43 ObsID59, with 10 Å binning.*

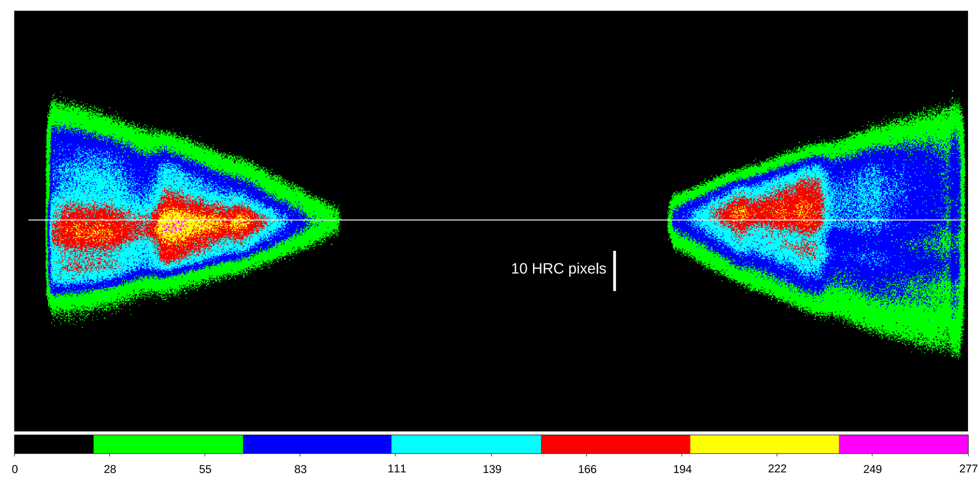

Figure 6: *Image of combined HZ43 spectra, after removal of tilts and wiggles. Horizontal axis is binned 200 times more than the vertical. The while horizontal line marks the median of the cross-dispersion profile.*

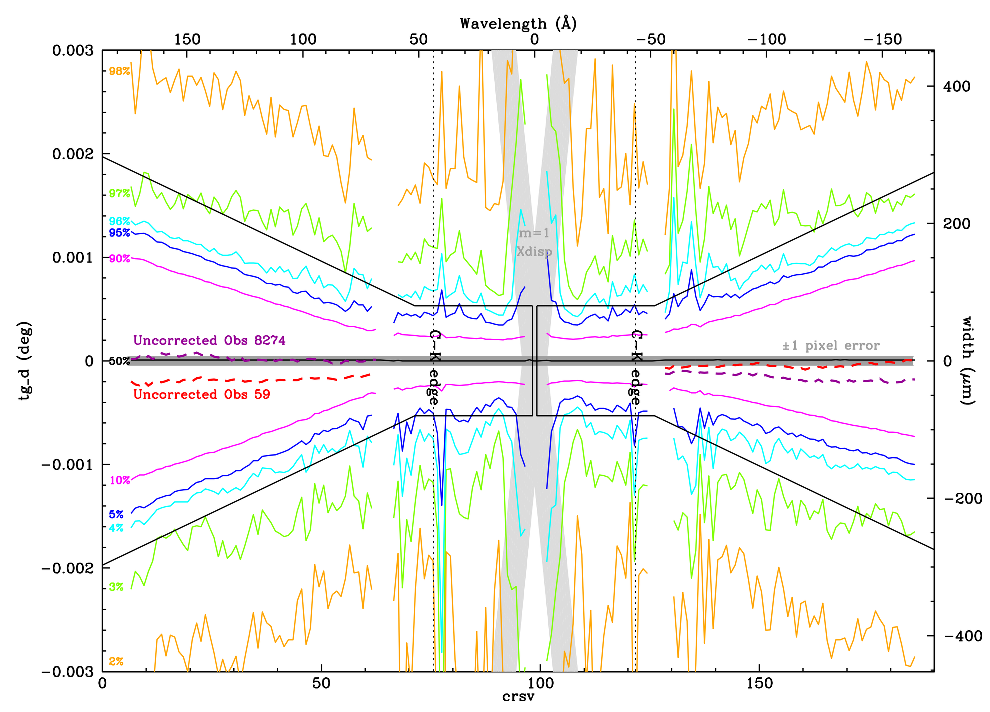

Figure 7: *Cumulative count fractions of corrected data from combined Mkn421 and combined HZ43 observations. The cross-dispersion 1st order is shown in light gray (also seen with 2nd order as the faint 'whiskers' in Fig. 1). Solid black line is the current spectral extraction region.*

As noted above, improvements to the determination of the 0th order position have already been implemented in the processing Pipeline. We will soon release contributed software for the other corrections, and are working to implement them in CIAO and the Pipeline. Corrections for time-dependent tilt can be made by adjusting a geometry file parameter and wiggle corrections can be made immediately after degapping using a lookup table. Current EEFRAC tables implicitly assume symmetry in the cross-dispersion profile and modifying the CALDB for use with an optimized (asymmetric) extraction region will require some effort. We will, in any case, provide a contributed software workaround.